

Defect detection in fiberglass reinforced epoxy composite pipes reproducing field inspection conditions

Most of the works that adopt active thermography as a non-destructive inspection method use very sophisticated equipment for test piece thermal excitation and data acquisition, which demand highly prepared operators, causing their application in industrial environments very costly. This paper aims at detecting defects in composite pipes by means of the Fourier transform phase angle analysis of the time evolution pixel amplitude, using simple and low-cost equipment.

Phase angle analysis is a well known technique, with a great potential in the area of thermography; being a kind of datum that is not difficult to obtain, it is less influenced by thermal excitation anisotropy and it allows measuring the depth of the defect, because the phase carries information about the thermal wave path. The Lock-in thermography can analyze, for a single frequency, the information contained in the infrared image, but it is not a technique easy to be repeated. Pulsed phase thermography allows the analysis of a series of frequencies by means of a single excitation, and it can be performed in a fast way. However, the equipment used in both techniques still represents some difficulty for a fast and reliable application in the industry, because of the high level of qualification necessary for the operators, as well as the high costs involved.

In this work, the method used was heating the test piece and then recording the temperature decay curve in the transient state of heat flow. Heating was performed in reflection using a hot air industrial blower and a high power halogen lamp. The only controlled parameters were excitation time and the distance from the exciter to the test piece. A Flir Prism Single Point infrared sensor was used in order to acquire the infrared images series. The test pieces were 60 x 80 mm and 6" pipe sections with 4mm thickness fiberglass reinforced epoxy containing circumferential defects with 5 to 10 mm of diameter and varied depths. A series of infrared images was recorded and a function corresponding to the time evolution of the thermal wave at pixel level was obtained during the cooling of the specimen. Then, it was possible to obtain the discrete Fourier transform of the temperature evolution of each pixel as well as the phase angle, $\Phi(\mathbf{u})$, given by equation 1.

$$\Phi(\mathbf{u}) = \tan^{-1}[\text{Im}(F(\mathbf{f}))/\text{Re}(F(\mathbf{f}))] \quad (1)$$

where $\text{Im}(F(\mathbf{f}))$ and $\text{Re}(F(\mathbf{f}))$ are the imaginary and real parts of the Fourier transform

The evolution of the phase angle in the frequency domain of several pixels of defective regions were compared with a pixel of a non-defective region, which was used as a reference through the difference between the values of the defect and the reference phase angles. There was a clear difference in the behavior of the phase angle variation between defective and intact regions, mainly at low frequencies.

Figures 1 and 2 show the phase angle difference graphics versus the frequency of two test pieces heated with the halogen lamp, showing the difference of behavior among phases for non-defective, visibly defective, little visibly defective, and invisible-to-the-naked-eye defective regions, in the infrared images.

In order to confirm the potentiality of the technique, defective regions that were not visible to the naked eye in any of the infrared images of the video were compared with the same previous reference (Figure 2-c); and, despite of the low amplitude, the difference in the behavior was once more noticed.

This result can also be used to establish a frequency for the composition of the phase images in order to precisely locate the little visible and invisible defects in the infrared images.

The preliminary results show the potentiality of the technique in the detection of typical composite pipe defects and support the realization of more tests aimed at the generalization of the results for other composite materials and other excitation forms.

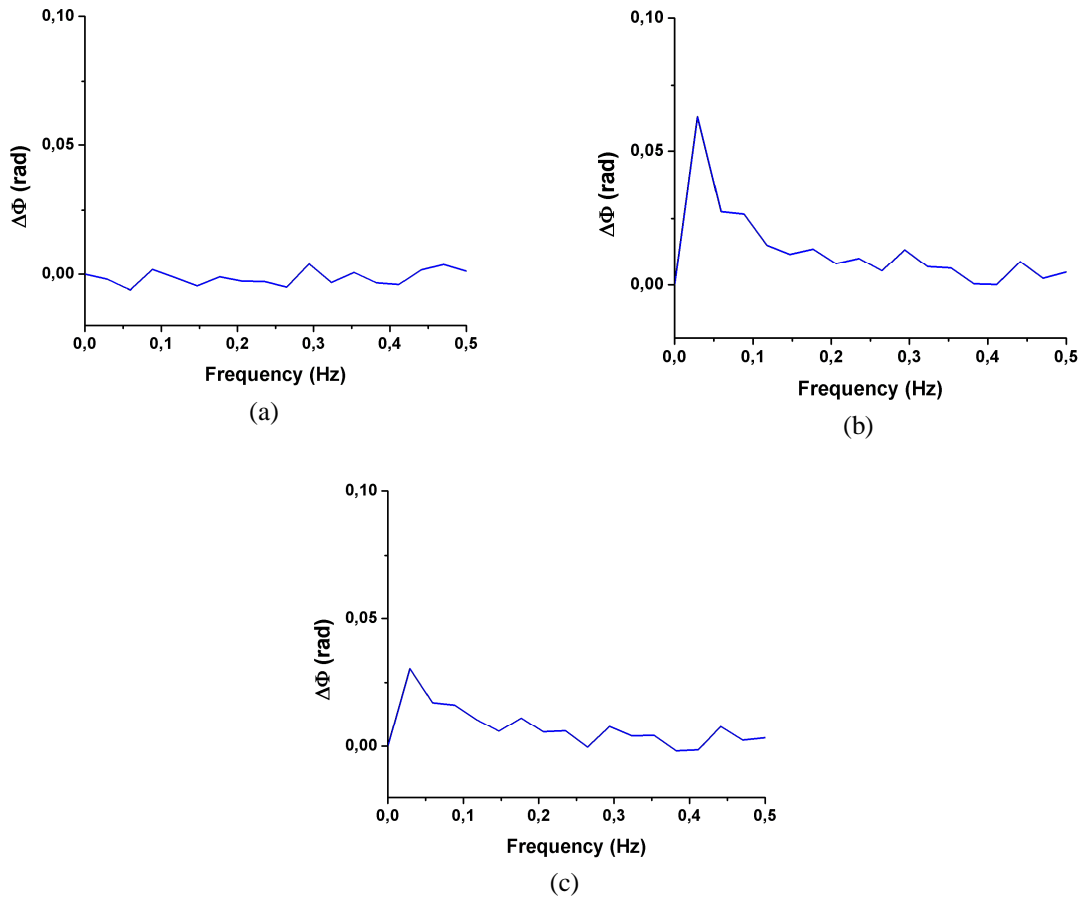


Figure 1 – Difference of phase angles: (a) non-defective region (b) region with 2,0 mm of depth defect visible in the thermogram (c) region with 1,5 mm of depth defect little visible in the thermogram

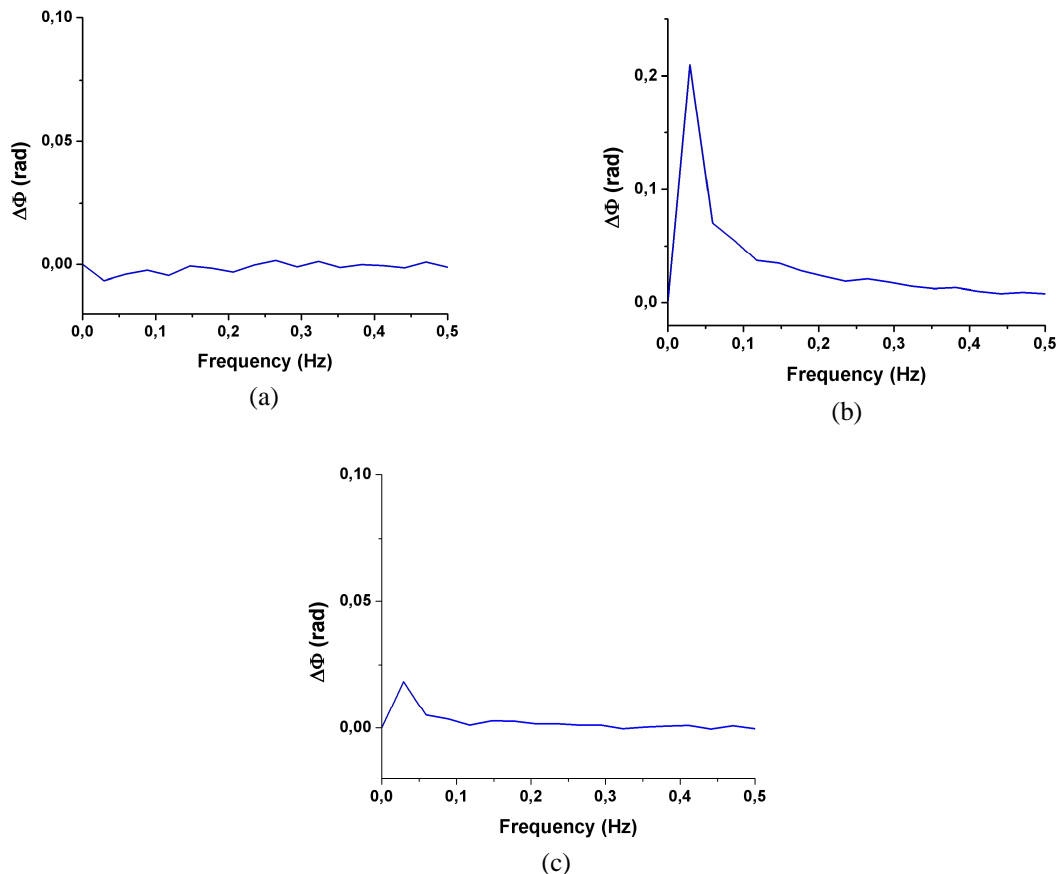


Figure 2 – Difference of phase angles: (a) non-defective region b) region with 2,0 mm of depth defect visible in the thermogram (c) region with 0,5 mm of depth defect non-visible in the thermogram